Contrast-Enhanced CT Imaging as a Non-Destructive Tool for Ex Vivo Examination of the Biochemical Content and Structure of the Human Meniscus

TABLE OF CONTENTS

GLOSSARY OF ABBREVIATIONS

CC2 Cysto-Conray II

CECT contrast-enhanced computed tomography

CT computed tomography

dGEMRIC delayed Gadolinium Enhanced MRI of Cartilage

DMMB dimethylmethylene blue

DOTA tetraazacyclododecanetetraacetic acid

DPTA diethylenetriaminepentaacetate

GAG glycosaminoglycan

HU Hounsfield unit

MRI magnetic resonance imaging

OA osteoarthritis

PMMA polymethyl methacrylate

ABSTRACT

Objective*:* Biochemical and biomechanical changes occur in the meniscus before osteoarthritis (OA) is clinically diagnosed through symptoms. However, existing techniques to characterize such changes are destructive and time-consuming. This study evaluated the ability of contrast-enhanced computed tomography (CECT) and contrast agent flux using the contrast agents Ioxaglate (ioxaglate) and CA4+ to correlate with the glycosaminoglycan (GAG) distribution and water content in *ex vivo* human menisci using microCT imaging.

Methods: A diffusion-in kinetics study for CA4+ was conducted to determine the equilibrium time for the contrast agents by subregion. Subsequently, the optimal concentrations of Ioxaglate and CA4+ to map the native GAG distribution were determined. Then, these optimal concentrations were used to examine correlations between CECT attenuation and GAG content at various time points, including equilibrium time. Using microCECT imaging, imaged zones were excised, rinsed, and analyzed for GAG content by subregion using the dimethylmethylene blue (DMMB) assay. Depth-wise analysis was performed through each of the native surfaces to examine differences in contrast agent diffusion kinetics and calculate flux. Finally, correlations between CECT attenuation and GAG content, CECT attenuation and water content, and flux and water content were calculated by subregion and whole meniscus.

Results*:* The equilibrium time was 48 hr with tau values ranging from 7.09 hr (posterior), 9.64 hr (anterior), and 12.32 hr (center). The optimal concentrations for native GAG mapping for ioxaglate and CA4+ were ≥80 mgI/mL and 12 mgI/mL, respectively. Using these optimal concentrations, weak to moderate correlations were found between ioxaglate CECT and GAG content at all diffusion time points, while strong correlations existed between CA4+ attenuation and GAG content as early as 7 hr (R^2=0.67), strengthening by equilibrium (R^2=0.81). CECT attenuation for both contrast agents did not significantly correlate with water content but CA4+ flux for the entire meniscus correlated moderately to strongly with water content (R^2=0.56-0.64).

Conclusions*:* CECT attenuation is a rapid, effective, non-destructive imaging technique to evaluate meniscal GAG distribution and water content. With CA4+ CECT, GAG content and distribution can be mapped in the human meniscus with high resolution. Consequently, CA4+ CECT is a useful tool for determining the biochemical health of human meniscal tissue, and further developments in quantitative imaging techniques will aid in understanding meniscal biology, diagnosis, and monitoring treatment outcomes.

INTRODUCTION

Meniscus and Osteoarthritis:

The human menisci are semilunar-shaped, weight-bearing fibrocartilaginous tissues [1]. Their function is to reduce friction in the knee joint, absorb shock, protect the articular cartilage from excessive stress during daily activities, and they are principally composed of water (70-75% by mass), collagens (20-25%), and proteoglycans (1-2%) [2, 3]. Various collagen types are present in the meniscus, including Type I [1], which typically has the highest concentration, and Types II, III, V, and VI [1]. They are arranged in internal bundles and tangentially to the tissue surfaces, providing the meniscus the ability to overcome the tensile and shear forces during locomotion, while the internal proteoglycans and their associated glycosaminoglycans (GAGs) hydrogen bond to water to confer meniscal tissue its compressive strength [2, 3].

Meniscal damage has been directly associated with osteoarthritis (OA), a degenerative joint disease affecting more than 27 million in the United States and 140 million worldwide [4]. The cost of osteoarthritis accounts for more than $125 billion in health care costs every year [4]. Osteoarthritis (OA) is a disease that affects structures that comprise the synovial joint, including the synovium, joint capsule, cartilage, meniscus and bone. While traumatic events can lead to meniscal tears, patients will often present with prolonged wear and tear degeneration of the meniscus rather than an acute injury [4]. Tears themselves can lead to inflammation and subsequent pain of the entire knee joint, leading to loss of range of motion. However, long before these gross morphological changes and symptoms are noticed, biochemical breakdown of meniscal tissue occurs [8]. Loss of glycosaminoglycans (GAG) renders increased cartilage permeability, allowing increased water flow, and thus softer and weaker cartilage [8, 10]. Furthermore, lower compressive and dynamic moduli are indicative of the cartilage's loss of ability to maintain structural integrity.

Biochemistry Assays

One reason for the high prevalence of OA is that it is often diagnosed long after irreversible changes in the articular cartilage and subchondral bone have transpired. This is because the diagnosis of OA is mostly empirical and patient-driven (pain, swelling, impaired function) and because current imaging modalities focus on morphological changes of cartilage which appear late in the course of OA. An effective and non-destructive imaging modality to

detect the early biochemical changes in cartilage is thus important for clinical and basic science purposes.

Biochemical assays and histopathological techniques have been employed to investigate such early changes in meniscal content and structure. The dimethylmethlyene blue (DMMB) assay [11] was developed to measure GAG content in tissues, including the meniscus. The assay has been successfully used to analyze regional differences in meniscal GAG content [2,5,12] and characterizing the role of cytokines including the effect of tumor necrosis factor (TNFα) on GAG depletion after meniscal injury [13]. However, this technique is destructive and time-consuming requiring the meniscus to be digested into smaller pieces, lyophilizing the tissue to obtain water content, digesting with enzymes, and plating dilutions of the digestion solutions with the DMMB dye. Another common technique that has been employed is Safranin-O staining of histological sections [5,12,14]. This method allows for visualization of areas with high GAG content but is also destructive and time-consuming, involving decalcifying and fixing the tissue for several days, which distorts the cartilaginous tissue matrix morphology [15]. Furthermore, embedding, sectioning and applying the stain further render the tissue permanently altered. Importantly, neither the DMMB assay nor the Safranin-O staining provides a 3D map of tissue GAG or water content.

Imaging

Given the limitations of these techniques, significant interest has been generated to develop alternative non-destructive means for characterizing and evaluating the meniscus ex vivo and in vivo. Various imaging modalities have been used to examine the meniscus, including plain radiography, MRI, CT and ultrasound [1,3,4].

Plain radiography is the most common modality used to evaluate patients with OA because of availability and low cost. However, only bone changes (subchondral volume loss, presence of osteophytes, joint space narrowing) can be detected with this method, because radiographs cannot be used to visualize soft tissues and only bone changes (subchondral volume loss, presence of osteophytes, joint space narrowing) can be detected.

Clinically, MRI is the gold standard for examining meniscus morphology, including detection of lesions, and for evaluation of treatment post-operatively, using both native and contrast-enhanced MRI [8]. Recently, with the development of delayed Gadolinium Enhanced

MRI of Cartilage (dGEMRIC), researchers have begun to investigate the use of dGEMRIC with the meniscus [8, 9]. dGEMRIC involves the use of diethylenetriaminepentaacetate (Gd-$DTPA^{2-}$), an anionic agent that helps to provide a qualitative measure of the glycosaminoglycan content in cartilage. Previous *in vivo* dGEMRIC studies have examined differences in the vascularized and avascularized zones of the meniscus [9], meniscal T1 relaxation times between osteoarthritic and healthy subjects [9], relationships between T1 relaxation times of the meniscus and articular cartilage within the same subjects [9], the gadolinium diethylenetriaminepentaacetate (Gd-$DTPA^{2-}$) enhancement kinetics in the menisci [8], and diffusion of gadolinium tetraazacyclododecanetetraacetic acid (DOTA) into the synovial space following intravenous injection [8]. However, no studies have examined correlations between meniscal biochemical composition and any of the MRI relaxation times. Thus with MRI, only a qualitative and relative assessment of the GAG distribution in the meniscus can be made. MRI is also hindered by high cost and long acquisition times, making it not suitable for screening studies.

Compared to CT imaging, MRI has a relatively low spatial resolution and there is a need for specialized pulse sequences and software programs. MRI is also hindered by the fact that patients with metallic implants are ineligible due to disturbances in the magnetic field created by the prosthetics. This is non-trivial considering the fact that many patients with cartilage degeneration also have had a history of arthroplasty and metallic implantation.

Many of these challenges associated with MRI can be resolved with use of contrast-enhanced computed tomography (CECT). In the absence of contrast-enhancing agents, CT is ineffective since cartilage by itself does not attenuate x-rays well [25]. But given a safe and effective agent for cartilage, the possibility of rapid and cheap image acquisition, powerful 3-D resolution capabilities, simultaneous bone and cartilage imaging, and lack of obstruction from orthopaedic implants exists with CT imaging. Unlike MRI, CT is relatively inexpensive and fast, has high resolution and does not require specialized pulse sequences. Although CT imaging uses ionizing radiation, modern CT scanners can maintain high resolution with lower radiation doses, particularly at acceptable levels for imaging the knee [23-26].

But due to the lack of effective contrast agents, use of plain radiography and MRI dominate current OA imaging. The anionic agents Ioxaglate and Cysto-Conray II (CC2) are the only FDA-approved CECT agents used for cartilage. These agents were designed for arteriography, precisely to enhance endothelium visualization. Nevertheless, these anionic agents

have been used by a handful of physicians and researchers for cartilage CECT to provide information about the GAG distribution in cartilage that is not available with radiography or MRI [29,30].

Previous Work and Current Project

Our lab has investigated ioxaglate in both bovine and human meniscus samples – showing significant but weak to moderate correlation strength: bovine (R^2 =0.51, $p<0.05$) and human (R^2 =0.49, $p<0.05$) [12,27]. This indicates that there is a need for a more sensitive technique to determine meniscal GAG content. Because cartilage GAG and ioxaglate/CC2 are both negatively-charged, inverse GAG profiles can be generated where high CT attenuation would indicate low GAG levels and vice versa. Thus high concentrations of these contrast agents are needed for the concentration gradient to override the electrostatic repulsion of anionic agents to GAG. This impacts cost and compromises safety in patients; thus these CECT agents are not widely used. While anionic and non-ionic contrast agents exist, no cationic contrast agent is currently used for CECT. Our lab has synthesized and developed a CECT agent *designed* to image cartilage: **a novel cationic contrast agent, which our group calls CA4+, that is attracted to the negatively-charged GAGs comprising ECM of chondrocytes, the cells in cartilage.**

Our lab members have already published results of robust pre-clinical studies with CA4+ [29, 35, 37, 38]. The kinetics and affinity of anionic and cationic CT agents to GAG relative to the anionic agents have been characterized in various tissues. *Ex vivo* animal experiments with articular cartilage from bovine patella-femoral joints and bovine menisci have documented that the CECT attenuation and thus the sensitivity of CA4+ for GAG is significantly greater than that of anionic contrast agents. Finally, the higher CT sensitivity of CA4+ over anionic contrast agents over a wide range of concentrations at a fixed time was documented [31]. Furthermore, CECT attenuation using CA4+ has also been shown to correlate strongly with the compressive modulus of cartilage using microCT imaging, thus demonstrating that CA4+ may prove to be a biochemical as well as biomechanical diagnostic tool [31].

In addition, previous meniscal CECT studies have looked only at CECT attenuation at a single time point ("static CECT"), while recent reports using bovine cartilage and ioxaglate have indicated the utility of CECT imaging at several time points ("dynamic CECT") for measuring

contrast agent flux, which is known to reflect differences in cartilage water content and permeability [31]. Thus opportunities exist for using CECT to examine these properties in the human meniscus.

In addition, our lab completed an *in vivo* study of rabbit knee articular cartilage with CA4+ and ioxaglate [31]. No cytotoxicity effects were observed when the contrast agent was delivered intra-articularly, confirming the safety of the CA4+ agent in mammalian models [Joshi]. In the rabbits, the kinetics study revealed that the concentration of ioxaglate in cartilage and joint space approached the same concentration [31]. In contrast, the concentration of CA4+ increased in the cartilage and decreased in the joint space, providing stronger contrast between cartilage and joint space [1].

This is the first project in our lab to investigate *ex vivo* human cadaveric tissue using ioxaglate and CA4+. The focus of this study is to compare static and dynamic CECT imaging with ioxaglate and CA4+ for assessment of GAG, water content, and flux of the human meniscus. Given the similar biochemical makeup but smaller size of human menisci to bovine menisci, our group hypothesized that (1) the diffusion time of the contrast agent into the meniscal tissue would be shorter than that of bovine menisci, (2) that a lower concentration of CA4+ than ioxaglate will afford CECT attenuations that reflect the GAG distribution in the human meniscus, (3) the static CECT attenuation following equilibrium exposure in CA4+ will more strongly correlate with the GAG content than that of ioxaglate, (4) contrast agent flux with both agents will strongly correlate with tissue water content, and (5) owing to electrostatic interaction with the fixed negative charge density induced by the GAGs, the ioxaglate contrast agent flux will be greatest through the external surface, while the CA4+ flux will be greatest through the tibial and femoral surfaces.

METHODS

Material/Specimen Preparation and Imaging:

Five medial and five lateral menisci were carefully excised from the knees of human cadavers (5 donors, 60% male, mean age: 42.3 yrs, age range 20-54, purchased from MedCure (Portland, OR)). Each meniscus was sectioned into three regions: anterior, central and posterior (**Figure SI-1a)** [2, 12, 26, 27] and all samples were frozen at -20° C in 0.9% saline with protease inhibitors, and antibiotics for later use. Specifically, GIBCO Anti-Anti stock solution, 5mM of

EDTA and Benzamidine HCl (Sigma S8820, St. Louis, MO) were included in all the solutions that were exposed to the menisci samples to prevent nonspecific degradation during the studies. Given the native osmolality of the meniscus, known to be between 350-400 mOsm/kg [12,28], we sought to maintain the osmolality of all solutions for all studies was maintained at 400 mOsm/kg by balancing the pH at physiological levels as well as titrating the osmolality with sodium chloride. Once thawing of each meniscus was complete overnight at 4° C, the non-native surfaces were sealed with cyanoacrylate glue to prevent contrast agent from diffusing through these surfaces. This would account for the fact that slicing the meniscus would artificially create non-native surfaces. This experiment consisted of three studies 1) a diffusion-in study to determine the time required for the cationic contrast agent (CA4+) to reach equilibrium, 2) an optimization study to determine the optimal concentration for CA4+ and ioxaglate by qualitatively comparing the ability of various concentrations of both agents to map the GAG distribution in human menisci at equilibrium, and 3) a fixed-concentration study a) to compare the CECT attenuation at different time points to tissue GAG and water contents and b) to compare the time-dependent contrast agent fluxes through each native surface to tissue water content.

Contrast-Enhanced Computed Tomographic (CECT) Imaging

For the diffusion-in study, three samples (one anterior, one central, and one posterior from 3 independent knees, **Table SI-1**) were immersed in 30 mL solutions of the CA4+ contrast agent [24] at 12 mgI/mL and imaged using microCECT at various time points up to 96 hr [12]. The time required for the contrast agent to reach equilibrium within the different regions of the meniscus was defined as the time after which the change in CECT attenuation per hour was less than 1% [12]. The diffusion-in CECT attenuation vs. time data was then fitted with an exponential function of the form $CECT\_attenuation = a*exp(-time/tau) + c$, where tau represents the time at which 63.2% of the equilibrium attenuation was reached [12].

The equilibrium immersion time was determined to be 48 hr from the CA4+ diffusion-in study. I assumed similar diffusion kinetics between CA4+ and ioxaglate for this tissue, given the similar diffusion-in kinetics of the two contrast agents for both articular cartilage [29] and the bovine meniscus [12]. Five new samples (**Table SI-1**) were immersed for 48 hr in 30 mL of 5 concentrations (12, 48, 72, 80, and 96 mgI/mL) of ioxaglate and imaged under the same scanning

parameters (see below). Samples were washed with saline for 48 hr, scanned to ensure thorough washout, immersed in 4 concentrations (6, 12, 24, 30 mgI/mL) of CA4+ for 48 hr, and then re-scanned. Two samples were immersed in the 12 mgI/mL concentration, because a previous bovine meniscus study showed this to be the optimal concentration for CA4+ [12].

From the results of the concentration optimization study, it was determined that immersing the samples to equilibrium in ioxaglate at concentrations of 80 or 96 mgI/mL best reflected the GAG distribution, so 80 mgI/mL was used in the final study given the simplicity of diluting the 320 mgI/mL stock solution. Similarly, CA4+ at 12 mgI/mL generated CECT color maps that qualitatively best reflected the natural GAG distribution in the human meniscus. Hence, this concentration was used for the final study.

For the final study, nine more samples (3 anterior, 3 central, 3 posterior, **Table SI-1**) were each immersed in 30 mL of ioxaglate solution at 80 mgI/mL for 1, 3, 5, 7, 9, 48, and 53 hr (to ensure early diffusion and equilibrium imaging data was captured) and subsequently imaged each time using microCECT. Samples were washed with saline for 72 hr and re-scanned to ensure complete desorption of ioxaglate. Then, the immersion, scanning and washout process was repeated with CA4+ at 12 mgI/mL. Following washout, the imaged zone was excised [12], lyophilized to measure water content, and analyzed with the DMMB assay to quantify GAG content (see below). For each time point, a mean CECT attenuation of the entire imaged zone (**Figure SI-1b**) of each meniscus region was measured (see below), and depth-wise attenuation profiles were generated perpendicular to each native surface (femoral, tibial, and external, **Figure SI-1c**). The CECT attenuation values were converted to contrast agent concentration using serial-dilution phantoms, the concentrations were fit with an exponential (same form as for the diffusion-in study), the first derivative was obtained from the fit at each time point, and flux values were computed [25] by multiplying the instantaneous rate of concentration change at each time point by the thickness from the outer edge to the center of the meniscus through each respective surface (the average of the three thicknesses was used to compute the fluxes for the entire region).

For all studies, each meniscus region was blotted to remove excess contrast solution and positioned in a microCT imaging system (μCT40, Scanco Medical AG, Switzerland) using a custom airtight holder that maintained a humid environment to prevent drying of the tissue. Sequential transaxial microCT images of the center of each meniscus section (imaged zone,

Figure SI-1b) were acquired at an isotropic voxel resolution of 36 μm, 70 kVp tube voltage, 113 μAmp current and 300 ms integration time [12]. The microCT image data were converted into DICOM format using Scanco's software and imported for post-processing into Analyze™ (AnalyzeDirect, Overland Park, KS). The meniscus was segmented using the "Auto trace" region-growing algorithm in the ROI module [12,35]. The mean CECT attenuation (HU) for each sample was obtained by averaging the attenuation values over all pixels contained within the imaging zone [12].

Histological Assessment

Histology was done on neighboring tissues of the meniscal samples of interest (**Table SI-1**). Specifically, the neighboring regions were immersed in a decalcifier/fixative solution (Formical-4, Decal Chemical Corporation, Tallman, NY), embedded in paraffin, and dissected into 5-μm pieces, sectioning parallel to the imaged zone of each sample. The sections were then stained for GAG distribution with 0.1% Safranin-O (S-2255, Sigma, St. Louis, MO) with 0.02% Fast Green (F7258-25G, Sigma, St. Louis, MO) following a standard procedure from www.ichworld.com [12,35]. Photomicrographs were captured at 5x magnification (Axio Imager 2, Zeiss Microscopy, Thornwood, NY) to determine the distribution of GAG in these samples [12,35].

Biochemical Assessment of GAG

The excised meniscus imaging zones from Study 3 were cut into three subregions (inner, middle, outer, **Figure SI-1c**) [2, 12]. The three segments were then lyophilized for 24 hours, and the dry weight of each sample was measured. After digestion in papain (1 mg/mL in 50 mM sodium phosphate, 5 mM EDTA, 2 mM DTT, pH 6.8) at 65 °C for 24 hours, the GAG content of each meniscus subregion was determined using the 1,9-dimethylmethylene blue (DMMB) colorimetric assay [11]. Briefly, each meniscus digestion solution was diluted 20 to 60 times for the assay. A linear calibration curve was generated using chondroitin-4-sulfate (Sigma 27042, St. Louis, MO) to convert from absorbance to GAG content. The absorbance of the standard curve and diluted digestion solutions at 520 nm was separately measured in triplicate using a plate reader (Beckman Coulter AD340, Fullerton, CA, USA). The total GAG mass of each sample was calculated using the calibration curve and normalized by the wet weight of the meniscus

subregion to determine the percentage of tissue GAG content. The weighted-average GAG content for each imaging zone was then calculated [12].

Statistical Analysis:

MATLAB was used to generate the exponential fit equations CECT_attenuation = a*exp*(-b*time)+c along with tau values. For statistical tests, linear regression analysis (SPSS v. 21.0.0.0, SPPS Inc.) was used to examine potential relationships between either microCECT attenuations or flux values for both agents and the samples' water and GAG contents. The coefficient of determination (R^2) was used to assess the strength of each correlation. Further, differences in flux values were compared between contrast agents and between native surfaces using one-way ANOVA. For all analyses, significance was set as two-tailed $p<0.05$.

RESULTS

Diffusion of CA4+ into Bovine Menisci Regions:

The CA4+ enhanced CT attenuation rapidly increased during the first ten hours of immersion for the diffusion-in samples, with the change in CT attenuation/hr eventually decreasing to <1% after 48 hr in all three regions of the meniscus. (**Figure 1**). Using CECT attenuation as a surrogate for contrast agent concentration in the meniscal tissue, the diffusion curves for all three regions (anterior, central, and posterior) were similar in shape, with the central region reaching a slightly lower equilibrium value. Fitting an exponential of the form CECT_attenuation = a*exp*(-b*time)+c) resulted in a mean tau value of 9.68 ± 2.62 hr (mean tau The individual tau values for the regions were calculated to be 7.09 hr (posterior), 9.64 hr (anterior), and 12.32 hr (center). The tau values represent the mean time at which 63.2% of the final attenuation was reached for all regions.

Optimal Ioxaglate and CA4+ Concentrations for Visualizing Meniscal GAG:

After immersing the meniscal sample in ioxaglate at 12 mgI/mL for 48 hrs, the CECT attenuation appeared relatively uniform with minimal differences observed in the itssue consistent with the contrast agent distributing uniformly throughout the tissue cross-section (**Figure 2a**). When the concentration was raised to 48 mgI/mL, the attenuation was greatest in the outer subregion of the tissue (**Figure 2b**). At 72 mgI/mL, the attenuation was greatest in the

center and the contrast agent appeared to be fully distributed within the tissue (**Figure 2c**). At the highest concentrations of 80 mgI/mL and 96 mgI/mL, the CECT attenuation appeared once again relatively uniform consistent with contrast agent being fully distributed within the tissue (with noticeably greater concentrations in the outer subregion (**Figures 2d &e**, respectively).

Following immersion in CA4+ at 6 mgI/mL for 48 hr, a slightly elevated CECT attenuation was observed in the inner subregion, although the CECT attenuation was the greatest in the inner and middle subregions (**Figure 2g**), consistent with the known GAG distribution in the bovine meniscus via histological analysis (**Figure 2j)** [12]. When the concentration of CA4+ was further increased to 24 mgI/mL and 30 mgI/mL, there was poor visualization of the GAG distribution, as the tissue appeared more uniformly enhanced throughout (**Figures 2h & i).** Safranin-O stained representative histological slices (**Figure 2j**) from neighboring tissues from the meniscal samples reflected the CECT images obtained following immersion in 80 mgI/mL ioxaglate and 12 mgI/mL CA4+ (**Figures 2d & g).** Hence these contrast agent concentrations were chosen as optimal for mapping GAG distribution and used for the subsequent studies.

CECT Attenuation vs. GAG Content as a Function of Immersion Time

The immersion time had a significant effect on the strength of the CECT vs. GAG content correlations for both contrast agents (**Table 1**). As time of immersion increased for both contrast agents, the R^2 values increased and the p-values decreased. For ioxaglate, R^2 values began at 0.01 at 1 hr and peaked at 0.44 at 53hr. However, none of these correlations were statistically significant. In contrast, for CA4+, R^2 values were both stronger and significant by 7 hr ($R^2>0.60$ and $p<0.05$). At the equilibrium time of 48 hr, the CA4+ CECT attenuation was strongly and positively correlated with meniscal GAG content, with GAG content accounting for 81% of the variation in CECT attenuation ($p<0.05$), compared to a R^2 of 0.38 ($p>0.05$) for ioxaglate (**Figure 3**).

CECT Attenuation and Contrast Agent Flux vs. Water Content

For both contrast agents, CECT attenuation did not significantly correlate with water content at any time points, although the R^2 values for CA4+ were all greater than those of ioxaglate (**Table 1**). However, contrast agent flux more strongly correlated with tissue water content than CECT attenuation for both agents. Specifically, for ioxaglate at 80 mgI/mL, the flux

for the entire imaging zone weakly to moderately correlated with water content ($0.04 \leq R^2 \leq 0.52$, $p>0.05$) (**Table 1, Figure 4a**), with the strongest correlation occurring at equilibrium ($R^2=0.52$, $p>0.05$). In contrast, CA4+ flux moderately to strongly correlated with water content ($0.34 \leq R^2 \leq 0.65$, **Table 1**), with the strongest and significant correlations occurring at early time points (1 – 9 hr, **Figure 4b**, all $p<0.05$) and weaker, not significant correlations at equilibrium ($R^2=0.36$, $p>0.05$).

Depth-wise Attenuation Profiles for the Three Native Meniscus Surfaces

For both contrast agents, depth-wise attenuation profiles were generated perpendicular to the three native meniscal surfaces (femoral, tibial, and external, **Figure SI-1c**) for all nine samples at each time point. Representative profiles for one sample (**Table SI-1**) are shown in **Figure 5**. When quantifying the average values across the depth-wise ioxaglate CECT attenuation at equilibrium (**Table 1**), the femoral and tibial surfaces were similar at 3013±299 (mean±SD) and 2778±377 HU, respectively, while the external surface had a greater CECT attenuation at 3237±255 HU, being significantly greater than that of the tibial surface ($p<0.05$). Similarly, for CA4+, the femoral and tibial surfaces were similar, at 1351±359 HU and 1258±302 HU, respectively. However, the external surface had a significantly lower attenuation at 927±325 HU relative to the femoral surface ($p<0.05$). Examining the change from the outer edge (sampled as the first five voxels of the profile) to the center (sampled as the last five voxels) for the samples after immersion in ioxaglate, all three surfaces had similarly shaped depth-wise profiles such that by equilibrium, there appeared to be a plateau (**Figure 5, top**) from the outer edge (normalized tissue depth = 0) to the center (normalized tissue depth = 1). After exposing the same samples to CA4+, the CECT attenuation values for the surfaces also plateaued at a greater value in the center relative to the edge at equilibrium, but the plateau formed at a greater tissue depth (**Figure 5, bottom**). Quantitatively, for ioxaglate, the percent increases in CECT attenuation at the center relative to the edge at equilibrium were 121%±12%, 132%±16%, and 117%±18% for the femoral, tibial, and external edges, respectively. With CA4+, the center was 203%±15%, 218%±46%, 247%±53% greater than the outer edge for the femoral, tibial, and external edges, respectively. The percent increases for CA4+ were all significantly greater than their corresponding ioxaglate values ($p<0.05$).

Flux by Surface Comparison between ioxaglate and CA4+

From the depth-wise attenuation analysis, flux values for each surface were calculated (**Table 1**). For both contrast agents, flux values were greatest at early time points, indicative of rapid diffusion after immersion. For ioxaglate, the femoral and tibial flux values were significantly less than those of the external surface at all early time points (1 hr – 9 hr, **Table 1**). For CA4+, there were no significant differences in flux values between the surfaces at the early time points (1 hr – 9 hr). Finally, all three surfaces had significantly different CA4+ flux values than ioxaglate flux values at the early time points (1hr – 9 hr, **Table 1**).

DISCUSSION

This study investigated the ability and sensitivity of CECT imaging using CA4+ and Ioxaglate to determine the GAG content and distribution in *ex vivo* human meniscus samples. Because lower levels of GAG are indicative of OA, and meniscal damage can contribute to the onset of knee OA, an imaging method for evaluating meniscal biochemistry, could enable early diagnosis of knee OA and prevent the progression of the disease. Furthermore, such a method could prove as a useful research tool to investigate new treatments with animal models without the need for harvesting animal joints.

The dimethylmethylene (DMMB) assay and histology are currently used to understand the biochemistry of the meniscus, but as described above, are both time-consuming and destructive techniques. And with imaging modalities, there exists an opportunity to obtain this information in a non-destructive way with contrast-enhanced CT (CECT) imaging.

Figure 1 shows the diffusion-in kinetics of our cationic contrast agent CA4+ into three distinct human meniscus regions. A relative equilibrium CECT attenuation ranging from 500 to 900 HU, depending on the subregion, was reached within 48 hr of diffusion in all subregions. Determining the steady-state equilibrium time for a substance into any tissue is important because only at the equilibrium time can it be assured that the tissue is fully saturated with the substance. Especially with tissues as fibrous as the meniscus, it is important to know the equilibrium time before any characterization of the immersed tissue can take place. Here, the 48 hr diffusion is consistent with results from previous CA4+ studies in our lab: the more fibrous bovine meniscus had a 96 hr equilibrium time and the thinner osteochondral specimens had a 24 hr equilibrium time [37]. This is also consistent with another previous study, which found that

the equilibrium time for ioxaglate was greater than 30 hr in the human meniscus, although the study was not carried out past this time point [27]. Furthermore, in articular cartilage the equilibrium diffuse time was between 8-24 hr [24, 29, 31, 36], and the tau values for the contrast agents were between 1.08 to 4.49 hr [24,29]. The meniscus equilibrium diffusion time and tau values are expected to be larger than this given the larger size and lower permeability due ot its heavily cross-linked collagen fibers, but also the human meniscus compared to bovine meniscus is expected to be smaller given the smaller size and higher permeability of the human meniscal samples compared to the bovine samples. However, the fibrocartilage human meniscus is not as permeable as osteochondral samples which is expected given the heavily linked collagen fibers around the surface of the meniscus likely limiting contrast agent diffusion [1]. Previous studies showed that the bovine had similar equilibration times amongst the subregions as well [12]. However, unlike the bovine meniscus where the equilibrium time was 95 hr with tau values of 20.6 ± 3.98 hr, the equilibrium time for the human meniscus was noticeably shorter with 48 hr with tau value of 9.68 ± 2.62 hr.

The contrast agent also appeared to initially diffuse through the proximal and secondarily through the distal surface, with little diffusion through the medial surface until times closer to equilibrium. This is likely due to the anisotropic arrangement of collagen fibers throughout the meniscus, with the tightest bundles located in the outer subregions [1]. Following intra-articular injection into an intact knee, the contrast agent would be exposed to the proximal and distal surfaces of the meniscus, thus permitting the agent to diffuse into the meniscal tissue.

After determining the diffusion kinetics, I sought to identify the optimal concentrations of both Ioxaglate and CA4+ to provide an accurate visual rendering, closest to that of the Safranin O-stained histology slide (**Figure 2j)**. In some sense, Ioxaglate served as the control relative to CA4+ because Ioxaglate is already FDA-approved and used by several surgeons and researchers to characterize meniscal GAG.

Color maps from CECT images of various meniscus regions immersed to equilibrium in various concentrations of ioxaglate, ranging from 12 to 96 mgI/mL, did not reflect the natural GAG distribution of human meniscus until the concentration surpassed 72 mgI/mL. At the low concentrations, Ioxaglate distribution was essentially homogeneous throughout the meniscus. Higher concentrations of greater than or equal to 80 mgI/mL (**Figures 2d & e**) showed increased signals in the outer region compared relative to the middle and inner subregion because of the

higher GAG concentration in the inner subregion. Thus an inverse representation of the GAG content, albeit crude, was revealed with ioxaglate at high concentrations whereas the optimal concentration to visualize the meniscal GAG for CA4+ was 12 mgI/mL, about seven to eight times lower than the concentration required for a similarly decent representation of GAG with Ioxaglate (**Figure 2g)**. CA4+ concentrations that were above the 12 mgI/mL threshold resulted in oversaturation and poor reflection of the GAG distribution, with difficulty in discriminating regions of high and low GAG (**Figures 2 h & i).**

This is consistent with previous studies which showed that in articular cartilage, Ioxaglate does not diffuse deeply into the tissue where the majority of the GAGs are concentrated, with only partial penetration into the deeper cartilage at concentrations even as high as 80 mgI/mL [25, 27]. The penetration of ioxaglate into the GAG-concentrated inner subregion is likely due to the lower concentration of GAG in this subregion (2-3%), compared to the greater concentration of GAG in the deeper cartilage tissue (4-6%). In the meniscus, while I observed good inverse representations of the GAG at 80 and 96 mgI/mL, these concentrations were significantly higher than those of CA4+, potentially leading to more toxicity effects from a pharmacological standpoint. The concentration of ioxaglate has to be increased to these high levels of 80-96 mgI/mL because only at these concentrations can the concentration gradient overwhelm the otherwise strong electrostatic repulsion of Ioxaglate to GAG.

With the cationic contrast agent CA4+, the GAG distribution could be readily observed. Although the CA4+ appeared to be fairly homogeneously distributed throughout the meniscus following immersion at the low concentration of 6 mgI/mL, immersions in concentrations of 12 mgI/mL reflected the natural GAG distribution in meniscus, with higher CECT attenuation in the middle and inner subregions than the outer subregion. Thus, effective GAG mapping of the meniscus was accomplished with similar concentrations of CA4+ as previously reported for use with bovine meniscus and cartilage.

Using 12 mgI/mL for CA4+ and 80 mgI/mL for Ioxaglate as the optimal concentrations for CECT imaging of the human meniscus, the next part of the study sought to determine how sensitive the CECT attenuation was for the GAG content at various time points (**Table 1)**. At times below 7 hours, including the 1 hr, 3 hr, and 5 hr time points that were tested, there were no significant R^2 values for either contrast agent. There was also no regular increasing progression of the R^2 values with time, likely due to the stochastic behavior of the contrast agent diffusing

into the tissue at early time points. For ioxaglate the CECT attenuation did not significantly correlate with GAG content. However, as shown in **Table 1**, the CECT attenuation with CA4+ significantly correlated with GAG as early as 7 hr ($R^2 > 0.60$). By equilibrium (48hr), ioxaglate still did not significantly correlate but the correlations were more pronounced ($0.38 \leq R^2 \leq 0.44$). This is contrast to a previous study of ioxaglate with the bovine meniscus where the correlation was significant ($R^2 > 0.51$, $p<0.05$) [12]. However, another study using a different imaging modality, a clinical cone-beam CT, showed that ioxaglate failed to correlate in the human meniscus. This may be a property of the human meniscus that is distinct from the bovine meniscus or that the bovine meniscus correlation with ioxaglate CECT is moderate at best. Of note, at equilibrium, CA4+ strongly correlates with GAG ($R^2 > 0.8$, **Figure 3)**. In the bovine meniscus, the correlation is stronger ($R^2 = 0.89$) [12], again possibly due to the inherent nature of the bovine tissue relative to the human tissue. However, this study clearly shows that a cationic contrast agent like CA4+ produces markedly higher and more significant correlations in the human meniscus, even at lower concentrations. This can be explained principally by the nature of electrostatic attraction of CA4+ to GAGs.

While static CECT attenuation, as measured by CECT attenuation at a given time point, correlated with GAG to varying degrees as discussed with ioxaglate and CA4+ at various time points, there was no significant correlation with meniscal water content at any time point **(Table 1)**. The water content was determined by lyophilization of the meniscus before the DMMB assay, which was used to quantify GAG content. This was important given that the immediate quantification of GAG via DMMB subsequent to lyophilization introduced fewer variables into the relative quantities of GAG and water, for instance, a delayed execution of the DMMB and thus loss of biochemical preservation of GAG following lyophilization.

Regarding static CECT attenuation and water content correlations, a previous study with the human meniscus showed weak correlations ($R^2 < 0.31$) between water content and ioxaglate CECT attenuation after 40 min [27] but only for one subregion, the lateral subregion, of the meniscus. Furthermore, another study showed similar, weak but significant, correlations with articular cartilage ($R^2 = 0.25$, $p<0.05$). Given the poor correlations with static CECT attenuation and water content, we sought to examine a "dynamic" variable, precisely the contrast agent diffusion or flux and its correlation with water content.

The plausible correlations with flux and water content were driven by the theoretical notion that water content was a surrogate for collagen density and intuitively could be expected to affect the rate of diffusion (flux). Our hypothesis was that the flux in comparison to any static CECT attenuation at any time would be more predictive of water content. We calculated not just flux across the whole meniscus but also individually across each of the three surfaces (femoral, tibial, and external). We observed that whole meniscus flux was most strongly correlated with water content, especially CA4+ flux (**Table 1)**. However, the correlations between ioxaglate flux and water content were weak to moderate (R^2 = 0.07-0.38, **Figure 4a**) and not statistically significant ($p>0.05$) until after 9 hr. In contrast, the correlations with CA4+ were much stronger (R^2 = 0.56-0.64) and significant ($p<0.05$, **Figure 4b**). It is expected that at early time points, the contrast agents diffuse most quickly given Le Chatelier's principle and the stronger equilibrium drive when one end of the concentration gradient has a much larger differential. As such, larger changes in attenuation are noted during early time points and the flux and water content are expected to have strong correlations at early time points. In fact, at equilibrium time points, the flux should poorly correlate with water content given the much strong attenuations at these time points. Our results indicate a somewhat surprising finding. With ioxaglate, the correlations are strongest at the equilibrium time points with poor correlation at early time points. In contrast, CA4+ has significant and strong correlations at early time points, as expected, but weaker correlations at equilibrium (**Table 1**). The stronger correlations for ioxaglate at equilibrium represents an anomaly, perhaps a mere coincidence as the flux has stabilized by that point. Thus using ioxaglate flux to predict water content, even though the correlations are stronger at equilibrium, may not prove useful. In contrast, the CA4+ flux is strongly correlated with water content at all the early time points. This indicates the usefulness of "dynamic" variables such as flux to predict tissue water content, an important characteristic of the meniscus.

There is notable lower ioxaglate flux across the femoral and tibial surfaces compared to the external surface at all time points, with the exception of equilibrium (**Table 1**), which described above may not be a reliable time point given the stabilization of flux. The increased flux through the external surface relative to the femoral and tibial surfaces is likely due to the composition of this surface, specifically the lower GAG content in the outer subregion of which the external surface comprises. This allows ioxaglate to diffuse more rapidly given that the GAGs are more concentrated centrally. With CA4+, this effect was not seen at significant. One

explanation for the lack of significance with CA4+ in this external region may be that the concentrations of CA4+ and ioxaglate are noticeably different, specifically 12 mgI/mL for CA4+ and 80 mgI/mL for ioxaglate. The larger concentration gradient for ioxaglate may explain the more rapid diffusion of ioxaglate through the external surface. I did not account for the use of same concentrations for ioxaglate and CA4+ given the failure of other contrast agent concentrations to depict GAG.

To illustrate the flux through each of the three surfaces, I sought to perform a depth-wise CECT attenuation from the respective surface edge to the center (**Figure 5**). With ioxaglate, the three surfaces all plateau by the time equilibrium is reached at 48 hr (**Figure 5-top**). The meniscus center was markedly increased attenuations at the center by equilibrium relative to the surface edge (121%±12% for the femoral edge, 132%±16% for the tibial edge, 117%±18% for the external edge). This made intuitive sense give the concentration of GAGs centrally and thus ioxaglate's electrostatic attraction to the center of the meniscus, lowering the relative attenuation for the surface edge. However, one previous study showed that by equilibrium, the surface edge tended to have higher attenuations even with ioxaglate and the fact that GAGs were concentrated centrally [27]. This was interesting given that the concentration of ioxaglate used was 48 mgI/mL and this study used 80 mgI/mL. While the electrostatics should be consistent, leading to a higher attenuation towards the center of the meniscus, it is possible in the outside study that the lower concentration of ioxaglate used at 48 mgI/mL prevented full penetration of the contrast agent into the tissue, precisely raising the question whether equilibrium was truly reached by the time the partitioning ratios < 100% in the study were calculated. When calculating the attenuation difference in the respective surfaces at equilibrium, there was statistical significance ($p<0.05$) as the external surface had attenuations of 3237±255 HU relative to the tibial surface of 2778±377 HU **(Table 1**).

However, with CA4+ the depth-wise attenuation profiles of all three surfaces plateaued deeper into the tissue **(Figure 5-bottom**). There were greater attenuations near the center relative to the surface edge (203%±15% for the femoral edge, 218%±46% for the tibial edge, 247%±53% for the external edge). This was likely due to the electrostatic attraction of CA4+ to the GAGs located centrally. The actual CECT attenuation mirrored this as the external surface had a lower CECT attenuation (927±325 HU) relative to the femoral surface (1351±359 HU, $p<0.05$) at later time points (**Table 1**). Since the external surface is furthest away from the inner GAGs and the

concentration of negative charges, CA4+ is expected to be of the lowest CECT attenuation at this surface relative to the other two surfaces. Interestingly enough, the increased percentage of central attenuation with CA4+ was almost double that of the decreased percentage of ioxaglate, despite CA4+ requiring 1/6 of the concentration of ioxaglate.

A notable limitation of this study includes the differing concentrations of CA4+ (12 mgI/mL) and ioxaglate (80 mgI/mL). While a rationale for this was given, precisely the ability to depict and map the GAG distribution, the differing concentrations becomes concerning when comparing flux values and their significance. Nevertheless, what is useful is the ability of the flux data to correlate with water content, regardless of the concentration. This reveals that dynamic variables, such as flux, is worth measuring when analyzing new imaging contrast agents. Here, the flux clearly correlates with water content, especially for CA4+ at early time points whereas the static CECT attenuation for CA4+ does not.

Another noteworthy limitation is that the equilibrium time of 48 hr is not clinically-relevant in the sense that it is too long to be used for clinical purposes. Yet it is at this equilibrium point where static CECT attenuation most strongly correlates with GAG content. The earliest time point at which correlation is observed is at 7 hr, which itself is also quite long. A possibility of reducing the equilibrium time is introducing mechanical convention to encourage the more rapid diffusion of contrast agent into the tissue. Furthermore, while static CECT attenuation may not correlate until higher values, **Table 1** reveals that as early as 1 hr, which is clinically-relevant, water content correlates with CA4+ flux. Diminishing water content of meniscal tissue is a clear biochemical change in osteoarthritis (OA) [9] and further studies should be pursued with water content and the severity of OA.

A third limitation of this study is the use of ex vivo tissue rather than investigating the meniscus in its native in vivo environment. While I predict that the composition of the meniscus does not change given our preservation with protease inhibitors and antibiotics, the native milieu of the meniscus including the synovial fluid, opposing synovium and articular cartilage can contribute to changes in the diffusion of the contrast agent. While the conditions when experimenting with *ex vivo* human cadaveric menisci are different from that of an intact *in vivo* joint space, several conditions were used to mimic the native environment. The constant submersion of the cadaveric meniscal tissues in 400 mOsm, similar to the native *in vivo* environment, ensured hydration and preservation of morphology. The meniscal regions had to be

sliced into anterior, central, and posterior regions to ensure that the imaged region fit into the microCT holder. Thus the meniscal regions were not imaged in a way that maintained their native geometry of the meniscus in the knee. However, the cross-sectional geometry was maintained because the cut ends were sealed with cyanoacrylate glue to ensure diffusion through only native surfaces. This technique is analogous to sealing the exposed circumferential edge of osteochondral plugs prior to immersion in contrast agents. The confined space of the native joint was also difficult to mimic with *ex vivo* experimentation but previous *in vivo* experiments in rabbits showed that CA4+ can fully diffuse in the tight knee joint space.

CECT has been used for investigating other intact joints in vivo as well as other ex vivo tissues with success [29, 30]; however, to fully understand the meniscus in its native environment especially in the context of OA, future studies with live animals are needed. Another future direction of this project can investigate simulated tears, including radial and longitudinal tears which occur in meniscal injuries. The GAGs can be exposed with such tears and the ability of the contrast agent to diffuse will be changed given this exposure. While we predict that this will diminish diffusion times, it is dependent on the nature of the tear. Given the difficulty to accurately simulate a tear and limited supply of cadaveric human meniscal samples, we chose not to pursue this at this time.

An important future direction will focus on mechanical testing and the correlation between compressive moduli and CECT attenuation. Biomechanical along biochemical changes occur in the meniscus and the compressive modulus would prove to be a useful variable to investigate in addition to the ones identified in this thesis. Once a standardized method of calculating compressive modulus is established, a three-way correlation between compressive moduli, GAG content, and CECT attenuation can be calculated. The compressive modulus testing could be done by some form of indentation testing with a PMMA mold handling individual meniscal samples. The indenter tip could probe the compressive stress of the sample given a strain. The slope of the stress over strain will give the Young's modulus for each sample. The compressive modulus is expected to correlate closely with the GAG content because it has been established that GAGs are the primary molecular component for meniscal elasticity. Because I have seen that CECT correlates with GAG with strong sensitivity in this project, I expect a similar correlation with CECT with the compressive modulus. This will prove useful to

not only diagnose the biochemical health but also the biomechanical robustness of meniscal tissue.

CONCLUSION

In osteoarthritis, both cartilage and meniscus progressively degrade, resulting in a loss of proteoglycans, increased hydration and fibrillation of the extracellular matrix [5,28]. These compositional alterations affect the tissues' functionality; hence an early diagnostic capable of monitoring biochemical changes within the tissues could enable earlier detection of OA before severe damage occurs.

This project has seen for the first time the use of CA4+ in *ex vivo* human tissue as well as investigating both static and dynamic CECT attenuation on properties including GAG and water content. Since CECT for OA diagnosis and evaluation of treatment is the ultimate clinical endpoint of this project, the methods and results in this study can hopefully be used in intact human joints and clinical CECT. Our group believes that CA4+ holds great promise as the first cationic CECT agent that is specifically designed for cartilage imaging.

Furthermore, the results in this study also suggest for the first time that CECT can detect the biochemical health of the meniscus at times far lower than the equilibrium time point (1 hr with flux, >7 hr with static CECT), providing encouragement for clinical implications. Additionally, since the subchondral bone in addition to the meniscus is thought to play a role in OA, CECT can simultaneously evaluate both soft tissue and bone, leading to a more efficient monitoring and diagnosis of knee OA.

While clinical use of CA4+ requires the success of further safety and efficacy studies, failure does not preclude the immense usefulness of CA4+ as a research tool. For example, CECT has the potential to substitute the DMMB assay, which many have considered to be time-consuming, inconsistent, and difficult to execute without proper conditions. In this study, the DMMB assay used triplicates to ensure reproducibility but was time-consuming. Utilizing CECT imaging to estimate GAG content would provide an easy and quick way for researchers to obtain an absolute GAG content to answer a variety of research questions, something dGEMRIC has been unable to do due to its limited ability to provide relative rather than absolute GAG levels in cartilage. Safranin-O and the DMMB assay are also relevant only in the setting of *ex vivo* tissues, since joints would have to be harvested and the techniques themselves destroy the tissue. Given

that CECT imaging is non-invasive, *in vivo* experimentation could be pursued on animal models, especially to investigate new treatments and the course of GAG degeneration in the context of OA degeneration.

In all, a successful CECT agent for cartilage will have an impact on the diagnosis and treatment for OA, benefitting the millions of patients who suffer from the common disease.

SUMMARY

This study invested the use of contrast-enhanced computed tomography (CECT) and contrast agent flux using both anion ioxaglate and cationic CA4+ in the human meniscus. The hope of the study is to effectively characterize GAG and water content of the meniscus in a non-destructive way given that the existing techniques such as dimethylmethylene blue (DMMB) assay and Safranin-O staining lead to irreversible changes in the meniscus. The ability to evaluate the meniscus in this way has implications for osteoarthritis (OA) given that such biochemical changes occur before clinical symptoms, at which point osteoarthritis is usually deemed irreversible.

The equilibrium time point for both contrast agents were calculated; then using this time, the concentration of the contrast agents were varied such that an optimal concentration for each contrast agent to visualize the native GAG against a Safranin-O control was determined. Finally, using the optimal concentrations, correlation with CECT and GAG content was made. With regards to dynamic CECT attenuation or flux, values were calculated with respect to each of the three native surfaces of the meniscus.

Strong and significant correlations were observed with CA4+ CECT and GAG content, and moderate correlations were observed the CA4+ flux and water content. All correlations with ioxaglate were weak or non-existent, revealing of the advantage that cationic agents such as CA4+ has for imaging negatively-charged GAG tissue such as that found within the meniscus.

While further studies are required to determine the use of CECT in native meniscal tissues, this does not preclude the use of CA4+ as a useful research tool given that it is non-destructive and efficient. Given the limitations of radiographs, ultrasound, MRI, CECT is a promising tool to understand the meniscus scientifically and clinically.

CONTRIBUTIONS AND ACKNOWLEDGEMENTS

I would like to thank Benjamin Lakin and Rachel Stewart for their help with the design of this study, Jonathan Freedman for the synthesis of the CA4+ contrast agent, and orthopaedic surgeon Dr. Martin Wieworski for contributions to the experiments and data interpretation.
I would like to thank Dan Grasso for the use of his imaging fixure, Suzanne White at the Beth Israel Deaconess medical Center Histology Core for sectioning and staining of the histology samples, and the Center for Advanced Orthopaedic Studies at the Beth Israel Deaconess Medical Center for use of their CT scanner. MWG and BDS have a conflict of interest as they have support from the NIH for this project and MWG has a patent submitted on the CA4+ contrast agent.

I would also like to thank my mentors Dr. Mark Grinstaff and Dr. Brian Snyder for their guidance, supervision, and support on this project.

FUNDING

This work was supported in part by the Coulter Foundation, the Harvard Catalyst Program, the NIH (R01GM098361), the Henry Luce Foundation (R.C.S), and the Harvard Medical School summer fellowship (D.J.O). M.W.G. and B.D.S. have a COI via a submitted patent application via the university (M.W.G.) and grant funding from the NIH (M.W.G. and B.D.S.).

REFERENCES

1. Mow VC, Huiskes R. Basic Orthopedic Biomechanics and Mechanobiology. 3rd Edition. Philadelphia, Lippincott Williams & Wilkins 2005.
2. Fithian DC, Kelly MA, Mow VC. Material properties and structure-function relationships in the menisci. Clin. Orthop. 1990: 19-31.
3. Ionescu LC, Lee GC, Garcia GH, Zachry TL, Shah RP, Sennett BJ, et al. Maturation state-dependent alterations in meniscus integration: implications for scaffold design and tissue engineering. Tissue Eng. Part A 2011; 17: 193-204.
4. Miller MD, Thompson SR. DeLee & Drez's Orthopaedic Sports Medicine: Expert Consult-Online, Elsevier Health Sciences 2014.

5. Sanchez-Adams J, Willard VP, Athanasiou KA. Regional variation in the mechanical role of knee meniscus glycosaminoglycans. Journal of Applied Physiology 2011; 111: 1590-1596.
6. Wilson CG, Vanderploeg EJ, Zuo F, Sandy JD, Levenston ME. Aggrecanolysis and in vitro matrix degradation in the immature bovine meniscus: mechanisms and functional implications. Arthritis Research and Therapy 2009; 11.
7. Hunter DJ, Zhang YQ, Niu JB, Tu X, Amin S, Clancy M, et al. The association of meniscal pathologic changes with cartilage loss in symptomatic knee osteoarthritis. Arthritis & Rheumatism 2006; 54: 795-801.
8. Mayerhoefer ME, Mamisch TC, Riegler G, Welsch GH, Dobrocky T, Weber M, et al. Gadolinium diethylenetriaminepentaacetate enhancement kinetics in the menisci of asymptomatic subjects: a first step towards a dedicated dGEMRIC (delayed gadolinium-enhanced MRI of cartilage)-like protocol for biochemical imaging of the menisci. NMR in Biomedicine 2011; 24: 1210-1215.
9. Baum T, Joseph GB, Karampinos DC, Jungmann PM, Link TM, Bauer JS. Cartilage and meniscal T2 relaxation time as non-invasive biomarker for knee osteoarthritis and cartilage repair procedures. Osteoarthritis and Cartilage 2013; 21: 1474-1484.
10. Weinstein SL, Buckwalter JA. Turek's orthopaedics: principles and their application. Iowa City, Lippincott Williams & Wilkins 2005.
11. Farndale RW, Buttle DJ, Barrett AJ. Improved quantitation and discrimination of sulphated glycosaminoglycans by use of dimethylmethylene blue. Biochimica et Biophysica Acta 1986; 883: 173-177.
12. Lakin BA, Grasso DJ, Stewart RC, Freedman JD, Snyder BD, Grinstaff MW. Contrast enhanced CT attenuation correlates with the GAG content of bovine meniscus. Journal of Orthopaedic Research 2013; 31: 1765-1771.
13. Voigt H, Lemke AK, Mentlein R, Schünke M, Kurz B. Tumor necrosis factor alpha-dependent aggrecan cleavage and release of glycosaminoglycans in the meniscus is mediated by nitrous oxide-independent aggrecanase activity in vitro. Arthritis research & therapy 2009; 11: R141.

14. Croutze R, Jomha N, Uludag H, Adesida A. Matrix forming characteristics of inner and outer human meniscus cells on 3D collagen scaffolds under normal and low oxygen tensions. BMC musculoskeletal disorders 2013; 14: 353.
15. Cole MB. Alteration of cartilage matrix morphology with histological processing. Journal of microscopy 1984; 133: 129-140.
16. Nogueira-Barbosa MH, Gregio-Junior E, Lorenzato MM, Guermazi A, Roemer FW, Chagas-Neto FA, et al. Ultrasound Assessment of Medial Meniscal Extrusion: A Validation Study Using MRI as Reference Standard. American Journal of Roentgenology 2015.
17. Roemer F, Guermazi A. Osteoarthritis Year in Review 2014: imaging. Osteoarthritis and Cartilage 2014; 22: 2003-2012.
18. Huysse WC, Verstraete KL, Verdonk PC, Verdonk R. Meniscus imaging. Semin. Musculoskelet. Radiol. 2008; 12: 318-333.
19. Gatehouse PD, Thomas RW, Robson MD, Hamilton G, Herlihy AH, Bydder GM. Magnetic resonance imaging of the knee with ultrashort TE pulse sequences. Magn. Reson. Imaging 2004; 22: 1061-1067.
20. Krishnan N, Shetty SK, Williams A, Mikulis B, McKenzie C, Burstein D. Delayed gadolinium-enhanced magnetic resonance imaging of the meniscus: an index of meniscal tissue degeneration? Arthritis and Rheumatism 2007; 56: 1507-1511.
21. Gatehouse P, He T, Puri B, Thomas R, Resnick D, Bydder G. Contrast-enhanced MRI of the menisci of the knee using ultrashort echo time (UTE) pulse sequences: imaging of the red and white zones. 2014.
22. Li W, Edelman RR, Prasad PV. Delayed contrast enhanced MRI of meniscus with ionic and non-ionic agents. Journal of Magnetic Resonance Imaging 2011; 33: 731-735.
23. Lusic H, Grinstaff MW. X-ray-Computed Tomography Contrast Agents. Chemical Reviews 2013; 113: 1641-1666
24. Palmer W, Guldberg RE, Levenston ME. Analysis of cartilage matrix fixed charge density and three-dimensional morphology via contrast-enhanced microcomputed tomography. Proceedings of the National Academy of Sciences of the United States of America 2006; 103: 19255-19260

25. Kokkonen HT Suomalainen J-S, Joukainen A, Kroger H, Sirolo J, Jurvelin JS, et al. In vivo diagnostics of human knee cartilage lesions using delayed BCT athrography. Journal of Orthopaedic Research 2014; 32: 403-412
26. Lakin BA, Grasso DJ, Shah SS, Stewart RC, Bansal PN, Freedman JD, et al. Cationic agent contrast-enhanced computed tomography imaging of cartilage correlates with the compressive modulus and coefficient of friction. Osteoarthritis and Cartilage 2013; 21: 60-68
27. Honkanen J, Danso E, Suomalainen J-S, Tiitu V, Korhonen R, Jurvelin J, et al. Contrast Enhanced Imaging of Human Meniscus Using Cone Beam CT. Osteoarthritis and Cartilage 2015.
28. Joshi NS, Bansal PN, Stewart RC, Snyder BD, Grinstaff MW. Effect of contrast agent charge on visualization of articular cartilage using computed tomography: exploiting electrostatic interactions for improved sensitivity. Journal of the American Chemical Society 2009; 131: 13234-13235.
29. Bansal PN, Joshi NS, Entezari V, Malone BC, Stewart RC, Snyder BD, et al. Cationic contrast agents improve quantification of glycosaminoglycan (GAG) content by contrast enhanced CT imaging of cartilage. Journal of Orthopaedic Research 2011; 29: 704-709.
30. Stewart RC, Bansal PN, Entezari V, Lusic H, Nazarian RM, Snyder BD, et al. Contrast-enhanced CT with a high-affinity cationic contrast agent for imaging ex vivo bovine, intact ex vivo rabbit, and in vivo rabbit cartilage. Radiology 2013; 266: 141-150.
31. Kokkonen HT, Makela J, Kulmala KA, Rieppo L, Jurvelin JS, Tiitu V, et al. Computed tomography detects changes in contrast agent diffusion after collagen cross-linking typical to natural aging of articular cartilage. Osteoarthritis and Cartilage 2011; 19: 1190-1198.
32. Adams ME, Muir H. The glycosaminoglycans of canine menisci. Biochem. J. 1981; 197: 385-389.
33. Chevrier A, Nelea M, Hurtig MB, Hoemann CD, Buschmann MD. Meniscus structure in human, sheep, and rabbit for animal models of meniscus repair. J. Orthop. Res. 2009; 27: 1197-1203.

34. Baumgarten M, Bloebaum RD, Ross SD, Campbell P, Sarmiento A. Normal human synovial fluid: osmolality and exercise-induced changes. The Journal of bone and joint surgery. American volume 1985; 67: 1336-1339
35. Lakin BA, Ellis DJ, Shelofsky JS, Freedman JD, Grinstaff MW, Snyder BD. Contrast-Enhanced CT Facilitates Rapid, Non-Deustrctive Assessment of Cartilage and Bone Properties of the Human Metacarpal. Osteoarthritis and Cartilage 2015.
36. Silvast TS, Jurvelin JS, Aula AS, Lammi MJ, Toyras J. Contrast agent-enhanced computed tomography of articular cartilage: association with tisue composition and properties. Acta Radiologica 2009; 50: 78-85.
37. Bansal PN, Stewart RC, Entezari V, Snyder BD, Grinstaff MW. Contrast agent electrostatic attraction rather than repulsion to glycosaminoglycans affords a greater contrast uptake ratio and improved quantitative CT imaging in cartilage. Osteoarthritis and Cartilage 2011; 19: 970-976.
38. Bansal P, Stewart R, Entezari V, Grinstaff M, Snyder B. Contrast Enhanced Imaging of Cartilage Reflects Changes in Both Water and GAG Content. Orthopaedic Research Society Annual Meeting. Long Beach, CA2011:1618.

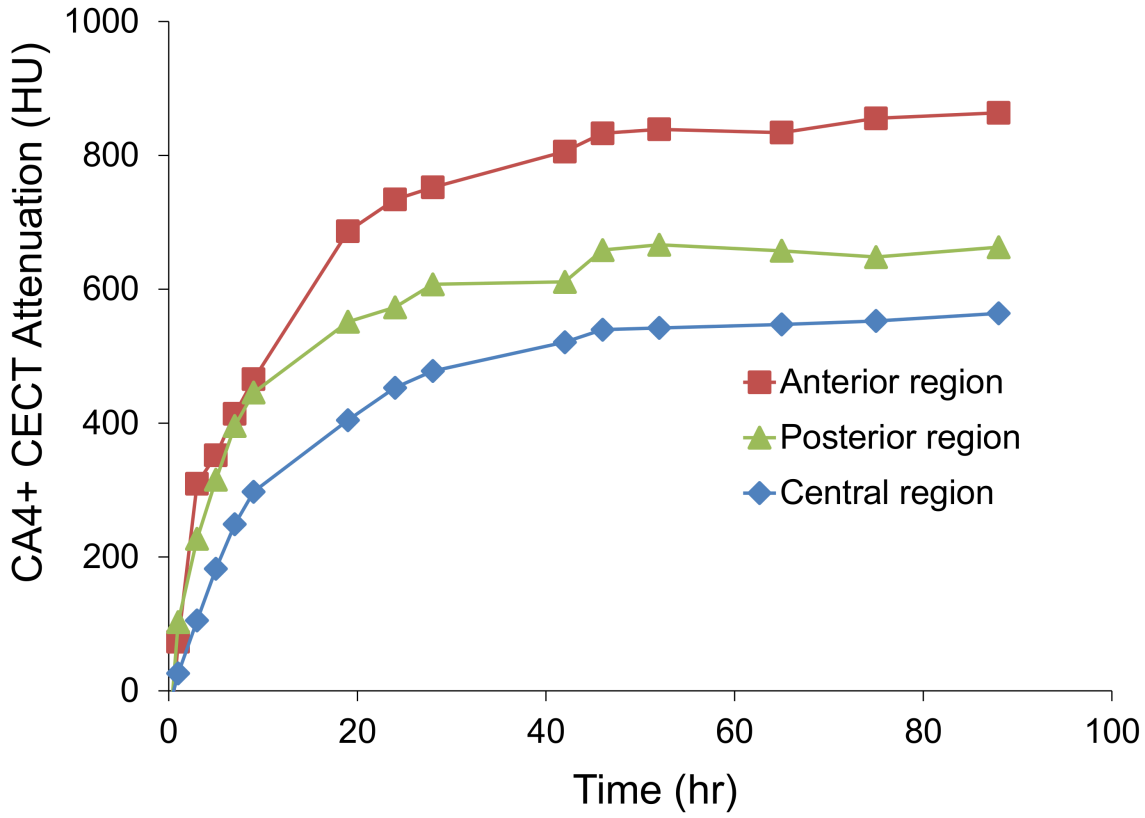

Figure 1: Diffusion-in curves for regions of three independent human meniscus samples. The state of equilibrium, defined as change in attenuation/hr being < 1% and visualized by a plateau, was attained by 48 hours.

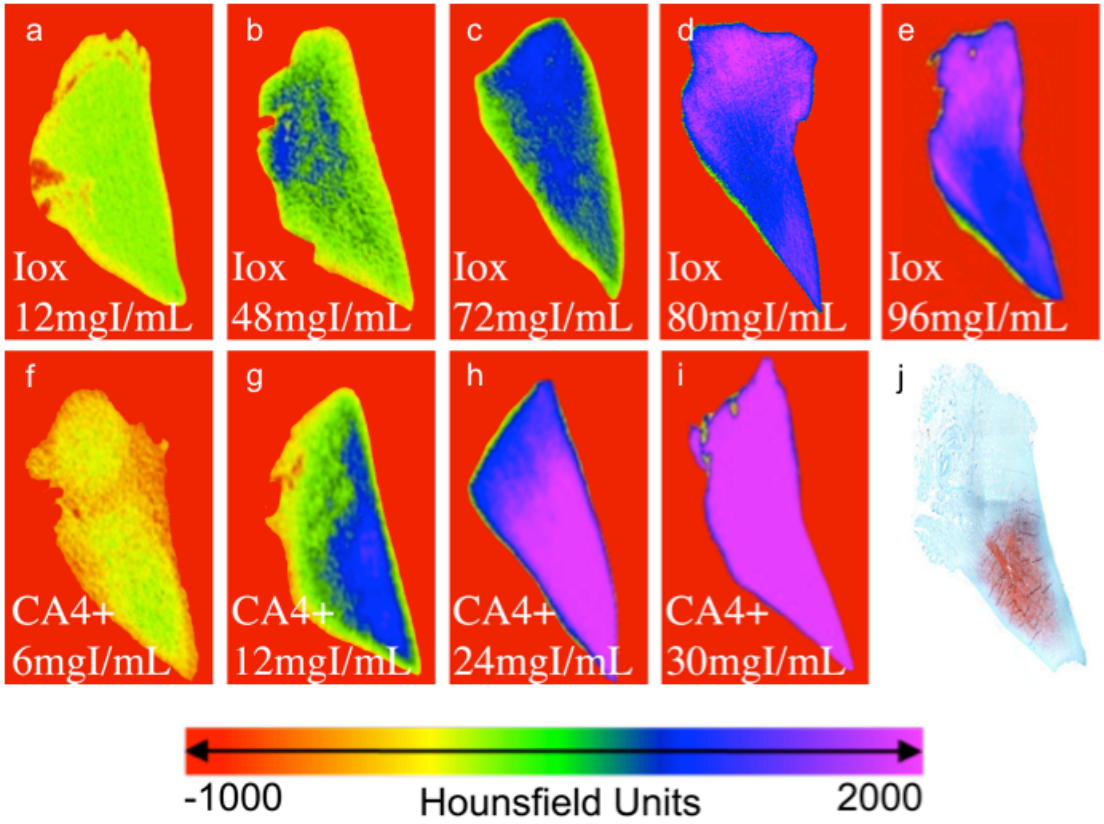

Figure 2: CECT color maps (from the center slice of the imaging zone) following equilibrium immersions of meniscal regions in varying concentrations of either ioxaglate (Iox, **a - e**) or CA4+ (**f - i**). A representative, neighboring Safranin-O histological (**j**) section was referenced to qualitatively determine the optimal contrast agent concentrations for Ioxaglate and CA4+. Optimal concentrations for visualizing the GAG distribution were found to be 80 mgI/mL for Ioxaglate (**d**) and 12 mgI/mL for CA4+ (**g**).

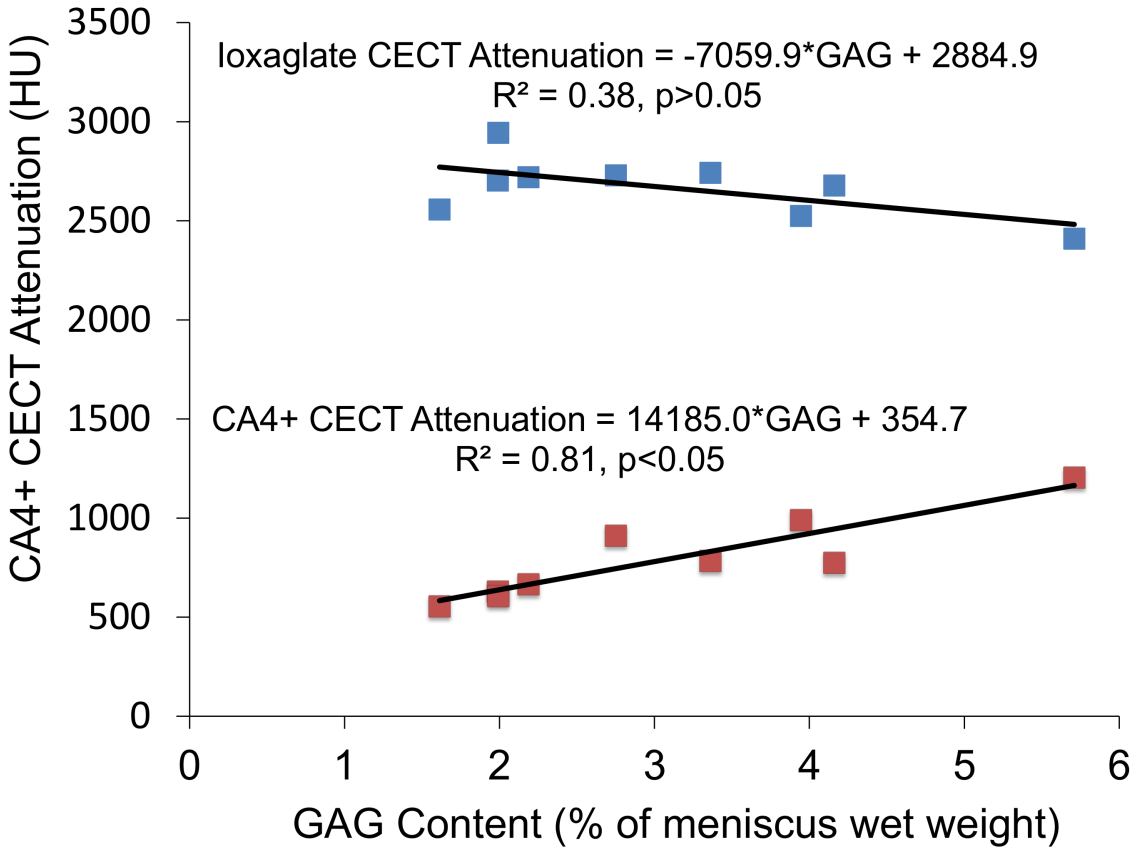

Figure 3: Linear regressions between CECT attenuation and GAG content after equilibrium immersion (48 hr) for the anionic contrast agent ioxaglate and the cationic contrast agent CA4+. The CA4+ enhanced CT attenuation positively and strongly correlated with GAG content (R^2 = 0.81, $p < 0.05$), while the correlation for ioxaglate was not significant (R^2 = 0.38, $p > 0.05$).

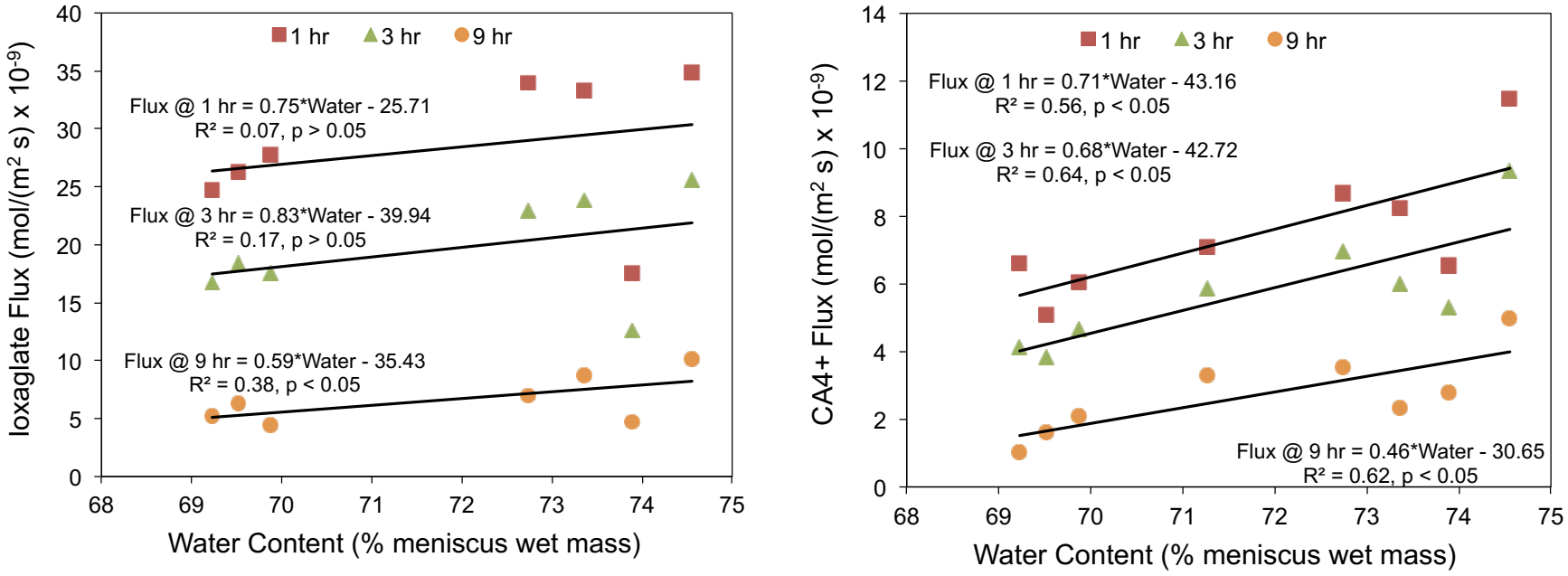

Figure 4: Contrast agent flux vs. water content for imaged zones (whole) after 1 hr (■), 3 hr (▲), and 9 hr (●) diffusion for: **a)** ioxaglate and **b)** CA4+ (note the different vertical axis scale). The corresponding correlations with CA4+ were moderate to strong (R^2 = 0.56-0.64) and significant ($p < 0.05$) while the 1-, 3-, and 9-hr ioxaglate correlations were weak to moderate (R^2 = 0.07-0.38) and not significant ($p > 0.05$).

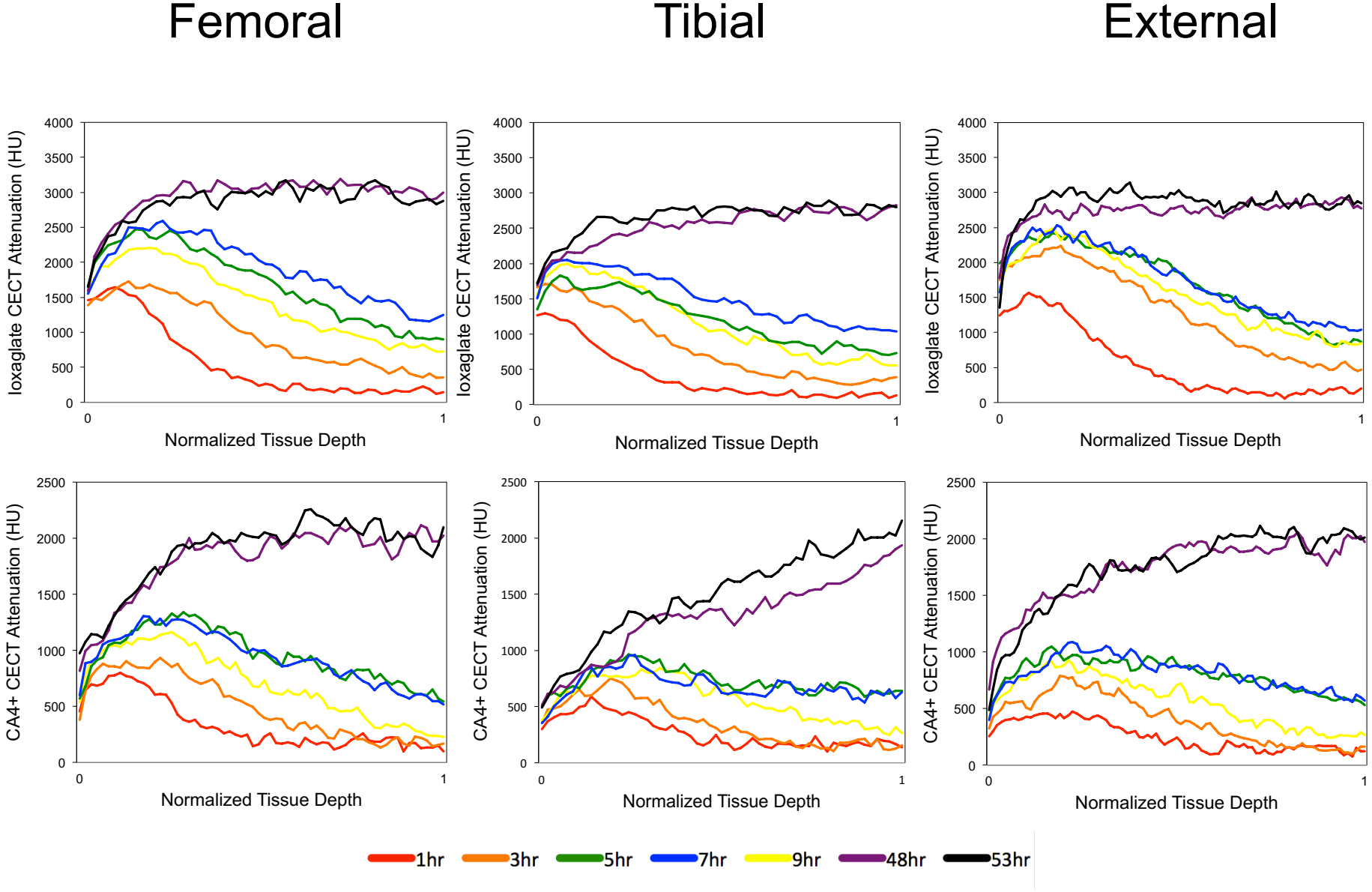

Figure 5: Depthwise attenuation profiles as a function of normalized tissue depth (from outer edge (depth = 0) to meniscus center (depth = 1)) for the three meniscal surfaces (femoral, tibial, and external) of one representative sample following exposure to either Ioxaglate (top row) or CA4+ (bottom row).

Ioxaglate (80 mgI/mL)

Time (hr)	CECT vs. GAG	CECT vs. Water	GAG vs. Water	Flux-Whole vs. Water	CECT Attenuation (HU)				Flux (mol/(m^{2}s) x 10^{-9})			
					Whole	Femoral	Tibial	External	Whole	Femoral	Tibial	External
0	-	-	-	0.04	0	0	0	0	35.1	23.5‡	24.0‡	53.9
1	0.01	0.06	-	0.07	729	500	539	611	31.1	19.8‡	22.0‡	49.0
3	0.02	0.06	-	0.17	1464	1065	1212	1248	22.2	15.9‡	16.3‡	33.2
5	0.20	0.07	-	0.25	1807	1372	1449	1762	14.8	12.5‡	11.7‡	21.7
7	0.14	0.02	-	0.33	2075	1653	1672	2125	10.1‡	9.20‡	8.49‡	15.2
9	0.22	0.07	-	0.38	2237	1934	1837	2344	7.09‡	7.07‡	6.44‡	10.8
48	0.38	0.15	-	0.52	2896	2904	2707	3166	0.010	0.0560	0.0734	0.0662
53	0.44	0.06	0.22	0.51	2931	2895	2745	3266	0.004	0.0310	0.0438	0.0382

CA4+ (12 mgI/mL)

Time (hr)	CECT vs. GAG	CECT vs. Water	GAG vs. Water	Flux-Whole vs. Water	CECT Attenuation (HU)				Flux (mol/(m^{2}s) x 10^{-9})			
					Whole	Femoral	Tibial	External	Whole	Femoral	Tibial	External
0	-	-	-	0.47	0	0	0	0	9.16^	7.82^	7.91^	11.6^
1	0.07	0.45	-	0.56*	219	199	187	128	7.90^	7.00^	7.09^	9.74^
3	0.22	0.46	-	0.64*	368	383	354	249	5.91^	5.64^	5.72^	7.03^
5	0.09	0.33	-	0.65*	519	561	522	417	4.67^	4.57^	4.65^	5.17^
7	0.67*	0.39	-	0.64*	534	617	584	470	3.06^	3.72^	3.80^	3.87^
9	0.60*	0.49	-	0.62*	666	718	701	558	2.62^	3.05^	3.12^	2.95^
48	0.81*	0.29	-	0.36	934	1233	1163	829	0.031	0.114	0.128	0.0846
53	0.81*	0.34	0.22	0.34	968	1263	1211	882	0.018^	0.0779	0.0897	0.0596

*Significant correlation ($p < 0.05$)

‡Significantly different than Flux-External for same contrast agent ($p < 0.05$)

^Significantly different than corresponding loxaglate value ($p < 0.05$)

Table 1: Summary table comparing properties and correlations for the same samples exposed to ioxaglate and CA4+ at indicated time points. Properties included: CECT Attenuation (HU) and flux values for the whole imaging zone, as well as through the femoral, tibial, and external surfaces. Correlations examined include: CECT attenuation vs. GAG content, CECT attenuation vs. water content, GAG vs. water content, and flux of the whole imaging zone vs. water content.

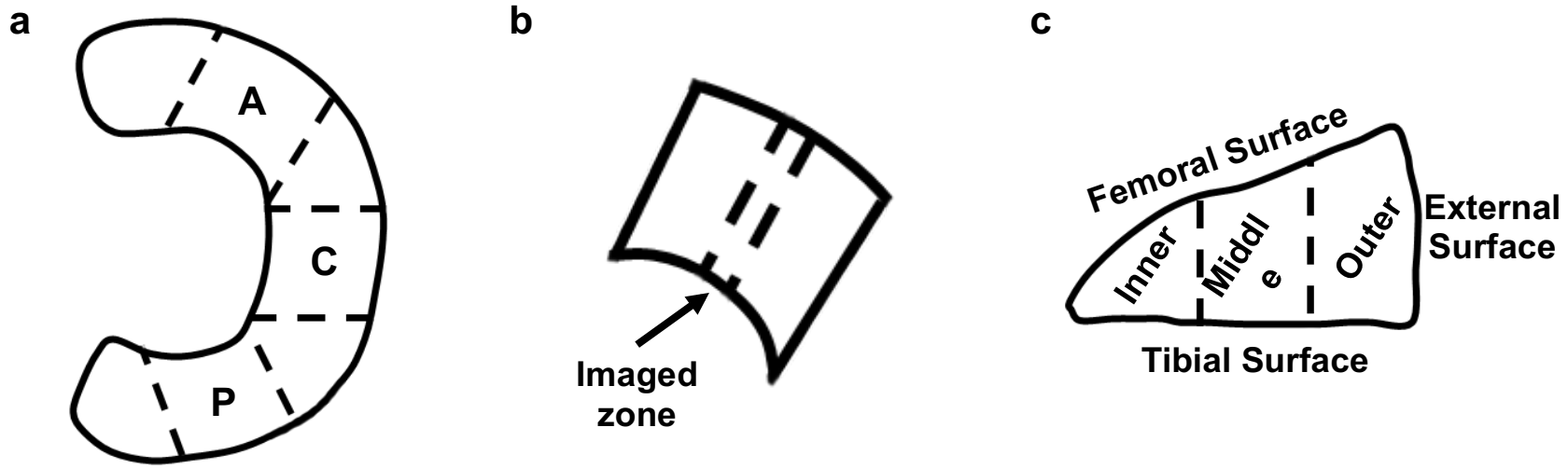

Figure SI-1: Preparation of the human menisci for CECT imaging and biochemical analysis. **a)** Schematic displaying how anterior (A), central (C) and posterior (P) regions were harvested from human menisci for all three studies. **b)** Location of CECT imaged zone in all regions that was also excised for DMMB assay to determine GAG content. **c)** Excised CECT imaged zones from samples in the fixed-concentration study were further divided into inner, middle, and outer cross-sectional subregions for determining GAG content in each subregion. Additionally, depthwise CECT attenuation profiles were generated perpendicular to each samples' native surfaces: femoral, tibial, and external (labeled in this schematic).

Knee Number	1						2						3						4						5					
Age	60						60						54						53						20					
Sex	Female						Female						Male						Male						Male					
Side	Medial			Lateral			Medial			Lateral			Medial			Lateral			Medial			Lateral			Medial			Lateral		
Region	A	C	P	A	C	P	A	C	P	A	C	P	A	C	P	A	C	P	A	C	P	A	C	P	A	C	P	A	C	P
Study 1: Diffusion-In Study (n = 3)																														
-Immersed in CA4+ at 12 mgI/mL		X						X															X							
Study 2: Concentration Optimization Study (n = 5)																														
-Exposed to Ioxaglate concentrations (mgI/mL) indicated													12	48	72	80	96													
-Exposed to CA4+ concentrations (mgI/mL) indicated													6	12	24	12	30													
-Neighboring tissued used for Safranin-O Histology														J		J*														
Study 3: Fixed-Concentration Study (n = 9)																														
-Immersed in Ioxaglate and then CA4+	X			X			X			X	X+														X	X	X	X		

A denotes Anterior region, C denotes central region, P denotes Posterio region, X denotes sample used for given study; X+ indicates sample for which the depth-wise attenuation profiles are provided in Figure 5; J* denotes sample for which neighboring tissue was sectioned and stained with Safranin-O and shown in Figure 2j; J denotes sample for which neighboring tissue was sectioned and stained with Safranin-O (not shown in Figure 2); For Study 2, numbers denote the concentration of the respective contrast agent in which indicated sample was immersed (as shown in Figure 2)

Table SI-1: Origin of meniscus samples (regions) for each study